Certain Investigation of the Retinal Hemorrhage Detection in Fundus Images

Ms.S.Deepa, Mr.S.Vijayprasath,*M.E.*
Department of ECE,
M.Kumarasamy College of Engineering, Karur, India

Abstract

Diabetic Retinopathy has become a common eye disease in most of the developed countries. It leads to damage of the retina, since fluid leaks from blood vessels into the retina. The presence of hemorrhages in the retina is the primary symptom of diabetic retinopathy. The number and shape of hemorrhages is used to indicate the severity of the disease. Early automated hemorrhage detection can help reduce the occurrence of blindness.Reliable detection of large retinal hemorrhages is important in the development of automated screening systems, which can be translated into practice. Our proposed work is to detect the large retinal hemorrhage detection part based on splat feature classification.Using fundus photographs the images are partitioned into number of splats. Each splat contains pixels with similar color and close spatial location. A set of distinct features was extracted within each splat. Following this, different features are extracted which serves as the guideline to identify and grade the severity of the disease. Based on the extracted features classification, the retinal image is distinguished as normal or abnormal using matlab codings.

Keywords*:* - Diabetic Retinopathy (DR), Fundus image, Retinal Hemorrhage, Splat feature classification.

I. INTRODUCTION

Automated detection of diabetic retinopathy (DR), as used in screening systems, is important for allowing timely treatment, and thereby increasing accessibility to and productivity of eye care providers [1]. Because of its cost effectiveness and patient friendliness, digital color fundus photography is a prerequisite for automated diabetic retinopathy detection [2]. Patients with images that are likely to contain DR are detected and referred for further management by eye care providers.

The most common signs of DR are microaneurysms, small hemorrhages , exudates, drusen, and cottonwool spots are located in the center of the macula. Two examples of large retinal haemorrhages are demonstrated in Fig. 1. Compared with anatomical strucutures , such as optic disc, fovea and blood vessels, the shape and appearance of haemorrhages show substainal variability in fundus images. Automated DR detection systems shows that an important cause of false negatives , as high as 50%, is formed by images that contain only large haemorrhages [3]. Large hemorrheges indicate more severe disease and improved detection of such lesions will lead to elimination of more severe of false negatives .

Small haemorrhages are regular in shape and many systems have been developed by this, and others to detect them [4]. A review of most recent work on hemorrhage detection can be found [7]. They primarily fall into three categories: pixel- based approaches, lesions-based approaches, and Image-based approaches. Pixel-based approaches focus on the location of haemorrhages on the retina. Lesion-based approaches use morphological Operations to define candidate lesions and count them.

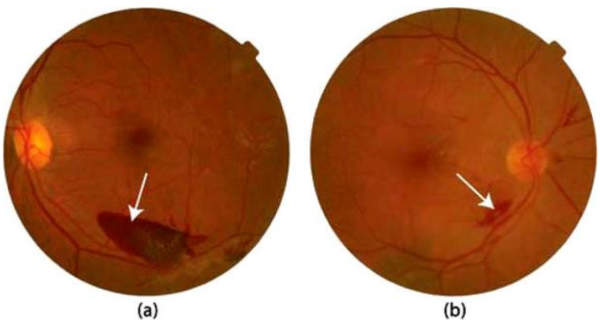

Fig.1 Examples of Retinal Hemorrhages with Different Hapes and Appearance

Image-based approaches are aimed at detecting images or eyes with haemorrhages. Large haemorrhages occur in frequently, and their appearances highly variable, making their shape modelling and automated detection a challenge. Detecting DR lesions is often accomplished by supervised classification, which involves training of classifiers using expert labelled target objects at pixel level [3].

Features are extracted from each pixel and soft labels are assigned accordingly, indicating the probability of the pixel being one part of a target object. Abnormal pixels are then combined into objects [8]. While their performance approaches that of clinicians, problems still exist.

- Ideally training samples are intended to be both informative to the classification model and varied so that information provided by individual samples overlaps as little as possible [9]. However, often in a single training image, there can be a huge number of very similar pixel samples.
- It is expensive to acquire labelled reference standards for training and evaluation. Designing such systems requires sustainably work by clinicians to define the reference standard, which is expensive and prone to error.
- Large haemorrhages occur frequently, have non-regular shape and occur without accompanying other signs of DR, such as microaneurysms or small haemorrhages. They will thus be missed by systems designed to detect regular DR lesions [8].

The following problems using a higher level entity the splat, which is a collection of pixels with similar color and spatial location. As hemorrhages consist of blood, they share appearance features with intravascular blood. That makes it difficult to differentiate these from retinal vessels using low level pixel features. On the contrary, by upgrading samples for classification from pixel level to splat level, with fewer disturbances from pixel level noise.

To overcome these drawbacks, in our proposed work to use the splat feature classification used to classify images for the following sections. In section II explores splat segmentation, section III describes the splat feature extraction and section IV presents splat classification and section V to evaluate the experiment results and section VI the following conclusions are made by using the MATLAB coding.

II. SPLAT SEGMENTATION

In splat based representation the image re-sampling strategy onto a irregular grid. Background regions, are gradual variations in appearance, tend to consist of fewer large splats while foreground consist of smaller splats. At pixel level, the distribution of hemorrhage pixels and non-hemorrhage pixels are imbalanced. Since hemorrheges are usually settled for a small fraction of the entire image [11]. Instead of including only similar background pixels for training, as many re-sampling methods do, a splat based approach to maximize the diversity of training samples by retaining all important samples foreground regions consist of a large number of smaller splats.

A. Scale-Specific Image Over Segmentation

Splats are created by over segmenting images using Water-shed or toboggan algorithms [10]. Conventional image over segmentation on a regular grid generates so called “superpixels” [12],[13], a similar concept to ” splats”. But superpixels are roughly homogenous size and shape, resulting in a lattice pattern [14]. In contrast, a splat-based approach divides images into a irregular grid. depending on the properties of target objects can be detected.

To create splats which preserve desired boundaries separating hemorrheges from retinal background, we perform a scale-specific image over segmentation in two steps. Due to the variability in the appearance of the hemorrhages, firstly we aggregate the gradient of the contrast magnitude at a range of scale of localisation of contrast boundaries and separating blood and retinal background. The maximum of these gradients over scale-of-interest (SOI).

B. Splat-Based Reference Standard Acquisition

Supervised algorithms require labelled samples by experts, but it is expensive to acquire such data [17], because substantial time is required to define irregular boundaries of hemorrhages. Any misalignment with true boundaries introduces noise at the training stage. Given the limited number of training samples, it has considerable impact on system performances. This problem can be rectified by using a splat based image formulation. So that we have to compared both pixel- based approach and splat- based approach methods.

For pixel level annotations are allowed to expert two types of haemorrhages. Large and small hemorrhages show in Fig. 2 (a) large hemorrhags are indicated by a few points along the boundaries and is applied to connect those discrete points as enclosed curves shown in cyan. Small haemorrhages are indicated by a single point shown as a green dot. Thus the noise content is very high. For splat level annotation shown in Fig.2 (b), this process is simplified substantially. Comparing both splat only performs a single click to indicate the hemorrhage part. As splat preserve hemorrhage boundaries , the resulting refence standard is less noisy. As a result indicates when “1” consist of haemorrhages splats and “0” consist of no hemorrhages splats.

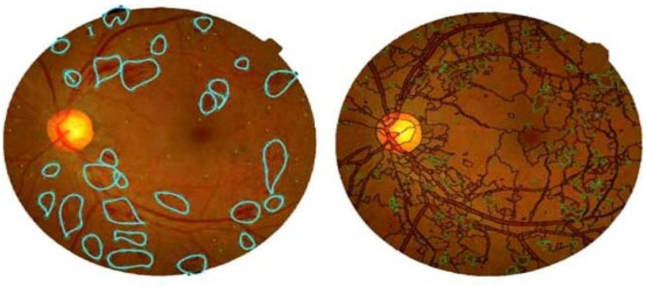

Fig.2 Sample Labelling Acquired from Expert Annotation with: (a) Pixel-Based Approach; (b) Splat-Based Approach

C. Edge effect Removal

As a pre-processing step, edge effects due to limited field of view(FOV) in fundus photographs [19] have to be proceeded to suppress feature extraction . This effect is visible in Fig. 3, It is performed only in two ways [20]. One is fill the region outside FOV with the mean color of the region within FOV. The other is to mirror the FOV outside the FOV. In Fig. 3(a) the clear edges still exist as the mean color is not necessary to blend faultlessly with the color on boundaries of FOV [20]. In Fig. 3(b) bright strips are visible on the left and dark strips on the right due to imperfections of illumination during imaging process.

III. SPLAT FEATURE EXTRACTION

Given splats with their associated feature vectors and reference standard labels, a classifier can be trained to detect target objects. In this method, two categories of features are extracted for splat–based hemorrhage detection as follows: 1) splat feature aggregated from pixel-based responses; 2)splat wise features (no aggregation is required).

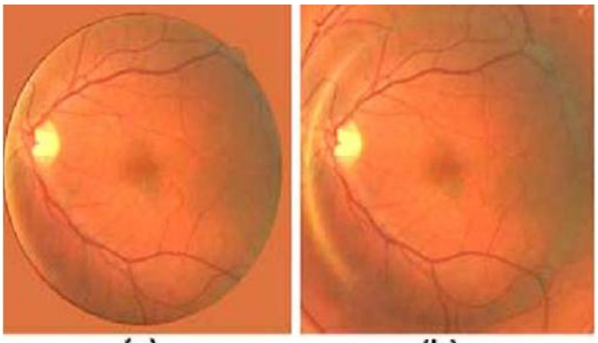

Fig.3 Splat Located on Field of View Boundaries are Excluded to Eliminate Edge Artifacts (a)Meancolor Background, (b)Mirror Circular Reflection

A. Pixel-Based Feature Response

The following features are as follows

1) Color Channel and Opponency Images

To accommodate color variations across the dataset, we normalise each image according to its dominant pixel level values at three color channels, which means most frequent pixel values present in the images are shifted to the origin of RGB color space. No separate rescaling is performed in order to preserve the ratio between color components. The color within each splat is extracted in RGB color space and dark-bright (db), red-green (rg), and blue-yellow (by) opponency images [21].

2) Characteristics of Boundaries Across Neighbouring Splats

To distinguish a structure or object from its surroundings or background, it is critical to differentiate distinct boundaries formed by neighbouring splats, such as well defined sharp boundaries resulting from sudden intensity transition, or blurred soft boundaries resulting from gradual intensity transition. It is also based on inside or outside and dark to bright or bright to dark. The high intensity points and low intensity points evolve towards different directions across the scale produced by Gaussian kernels with different symbols [22]. Different of Gaussian (DOG) are applied at five different smoothing scales and bandwidth of the boundaries present in the fundus images.

3) Response from Other Filter Bank

A Schmid filter bank [24] consisting of invariant kernels, is applied to dark-bright opponency images. Local texture filters including local range filter, local standard deviation filter and local entropy filter which compute the intensity range, standard deviation and entropy of one pixel in a given neighbourhood or region [25]. Dominant orientation and strength from steerable filters are applied to dark-bright opponency images [26].

B. Aggregation of Pixel-Based Responses

The way in which the splats are created so that the hemorrhages boundaries are preserved accurately, splat features images exhibit high intra-splat similarity and low inter-splat similarity between target classes.

To find the optimal strategy to aggregate pixel responses within each splat and associate it with a single feature value, two approaches are used, resulting in four sets of features. In the feature images, each splat is assigned a single value represented as intensity of that splat. The following features are to identity the hemorrhages splats. The mean splat responses from DoG filter bank show good separability between blood and non-blood splats. The SD splat responses show good separability between optic disc and the rest of the retina.

1) Splat-Wise Features

The extracted splat features need not to be aggregated. Shape features, such as splat area, extent, orientation and solidity, are derived based on individual splat distribution. Texture features are extracted according to the statistics of gray-level co-occurrence matrix (GLCM) [25].The list of splat features are summarised in table I. Each feature is normalised for all samples to have zero mean and unit variance. To build an effective classifier, it is crucial to extract discriminative features modified to target object [5]. The feature extraction process is to include as many potentially relevant features or which aggregation strategy are used to identifying hemorrhages splats.

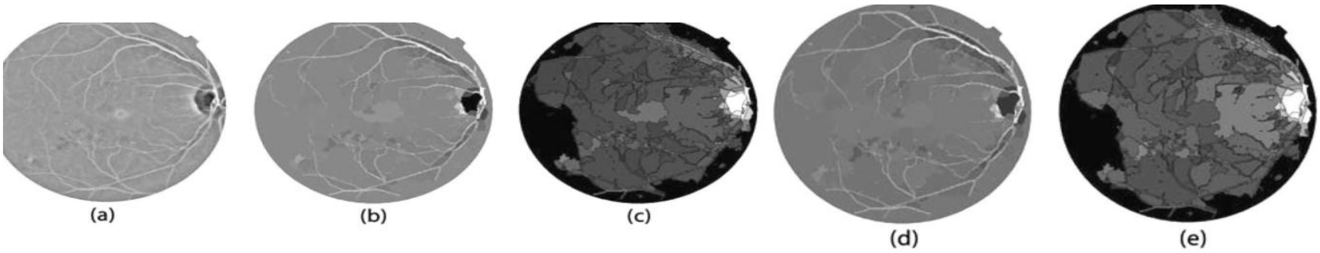

a)Difference of Gaussian Response Image from Green Channel , b) Mean Response Within Splat , d)Mean Response e)Standard Deviation

Table 1 List of Splat Features

Splat Area	Number Of Pixels In Splat
Splat Extent	Proportion Of Pixels In Bounding Box That Are Also In Splat
Splat Orientation	Angle Between Horizontal Axis And Major Axis Of The Ellipse As Splat
Splat Solidity	Proportion Of Pixels In Convex Hull That Also In Splat
Texture	Statistics Of GLCM
Color	RGB And Dark Bright , Red Green, Blue Yellow, Opponency
DoG Filter Bank	RGB And Db, Rg, By, Opponency
Gaussian Filter Bank	Used By Gaussian Filters
Local Filter Bank	Entropy Of One Pixel Neighbourhood, Db, Opponency
Steerable Filter Bank	Dominate Orientation And Strength

IV. SPLAT FEATURE SELECTION AND CLASSIFICATION

A. Two-Step Splat Feature Selection

o reduces the dimensionality of feature space by identifying relevant features and ignoring those irrelevant or redundant ones [30]. There are two approaches for the feature selection method: a) filter approach b) wrapper approach [30]. The filter approach is fast, enabling their practical use on high dimensional feature spaces. It assesses individual feature separately without considering their interactions. The wrapper approach assesses different combination of feature subsets modified to a particular classification algorithm at the cost of longer computation time. To use both the approaches for the feature selection process –a filter approach followed by a wrapper approach. The dataset are partitioned into a training set and testing set. It evaluates the discriminative power of candidate features according to the reference standard labels of training set as the input to a classifier.

1) Preliminary Feature Selection with a Filter Approach

This is to exclude those individual features that are not effective or irrelevant in separating hemorrhages and non-hemorrhages splats It is based on general characteristics to evaluate and select related feature subsets without involving any chosen induction algorithms [30]. The error on the testing subset increases while the error on the training subset decreases. The appropriate number of features to be retained is determined by using misclassification error (MCE).

2) Feature Selection with a Wrapper approach

After preliminary selection, irrelevant features are removed. By taking the interactions among the features into account, a wrapper approach selects optimal combinations of relevant features are minimized. It depends upon the classification algorithms. A k-Nearest Neighbor (kNN) classifier is used for this purpose.

B. 4.2 K-Nearest Neighbor (kNN) Classification

After feature selection, a trained KNN classifier is set up in a "calibrated" feature space with a discriminative features . The kNN classifier assigns soft class labels based on the k nearest neighbours in the feature space, i.e., those instances in the training set. When n neighbours were labelled as being a hemorrhage splat, the query splat comes from hemorrhage itself p was determined by p=n/k. The distance for finding the nearest neighbours is measured with Euclidean metric in optimized feature space [31]. At the testing stage the system is fully automatic. The k nearest neighbor rule attempts to estimate the posterior probabilities from labeled training samples [31]. A large value of k is desirable to obtain reliable estimates. But only when all of the k nearest neighbors are close enough to the query sample, it's a posterior probability can be approximately by the majority labels of its neighbors. Therefore, a compromise has to be made so that the value of k accounts for only a small of the training samples [31].

V. SIMULATION RESULTS

The experiment results have shown in figure 4. Using the input images the output images are extracted by using the segmentation, extraction and classification process. First the input image is loaded; the gradient filters are made based on the watershed segmentation. After finished the segmentation process, the noise is extracted by using the splat feature extraction method. Texture features are extracted according to the statistics of gray-level co-occurrence matrix (GLCM). Further the features are classified by using two filters banks i.e., DoG filter bank and steerable banks are used. Finally, the KNN classification is used as a trained classifier to classify the images and also detected the hemorrhages part.Similarly, several images have to be taken and get output i.e., hemorrhage part is detected by using the following algorithm.

The following diagram explains about the features of diabetic retinopathy.The above diagram describes about how the output image can be filtered out by the patient input image. From this input image, oriented filter image and steerable filter image can be obtained.

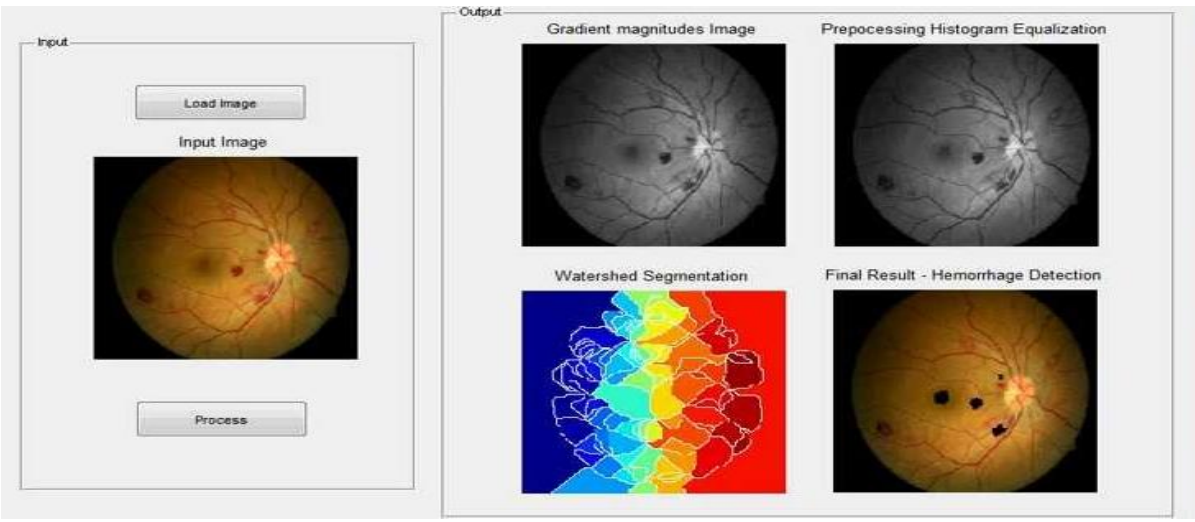

Input image

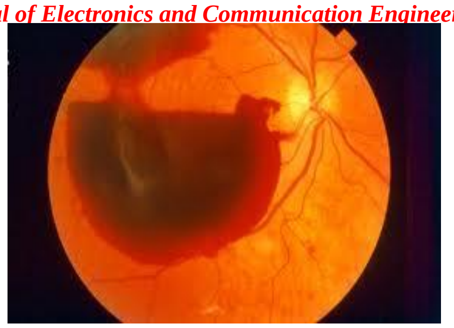

Output image

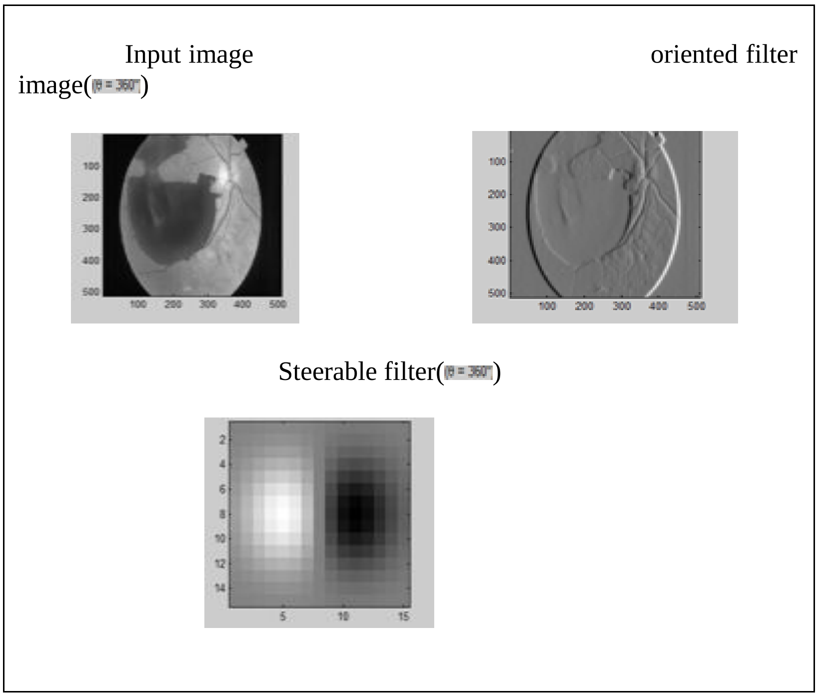

The following diagram explains the features of diabetic retinopathy. The affected part is located inside the retina ,from this filtered image the output part can be detected and results can be obtained.

Input Image

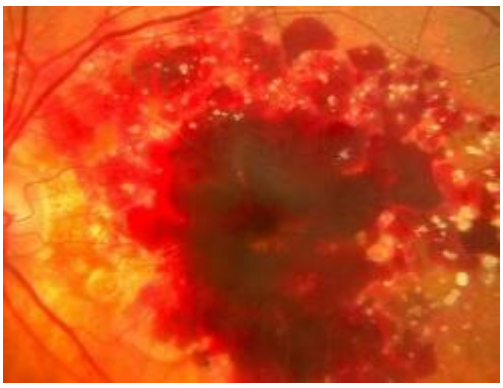

Output image

Input image

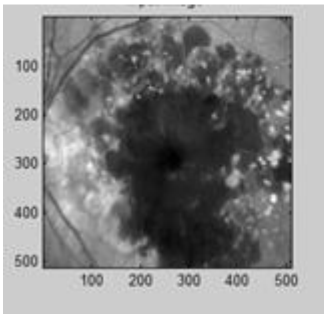

oriented filter image(θ = 360°)

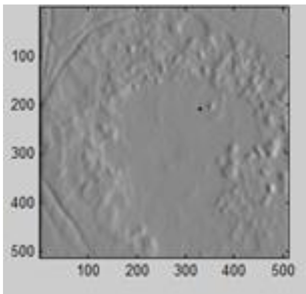

Steereable filter (θ = 360°)

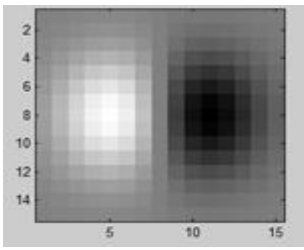

From this image, the infected part is located at the above region and results can be obtained by using this filtered image.The output image can be rotated around 360 degree and to find this affected part.

Input Image

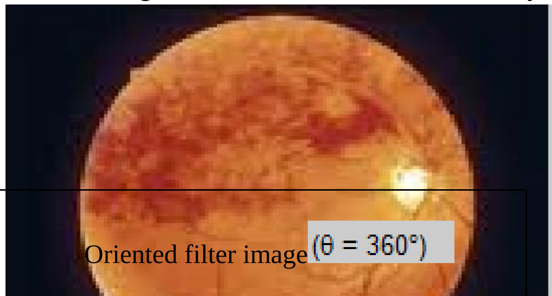

Output image

From the above diagram, this also one type of the diabetic retinopathy.The affected part is identified above the upper part of the retina.

Input Image

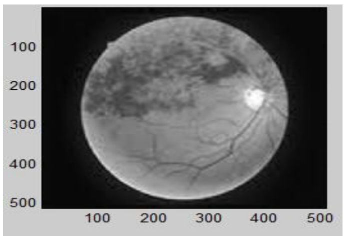

Oriented filter image (θ = 360°)

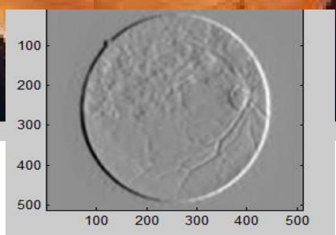

Steerable filter (θ = 360°)

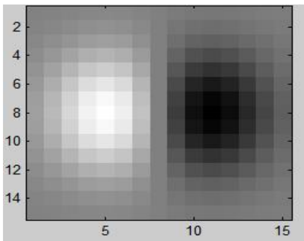

Input image

Output image

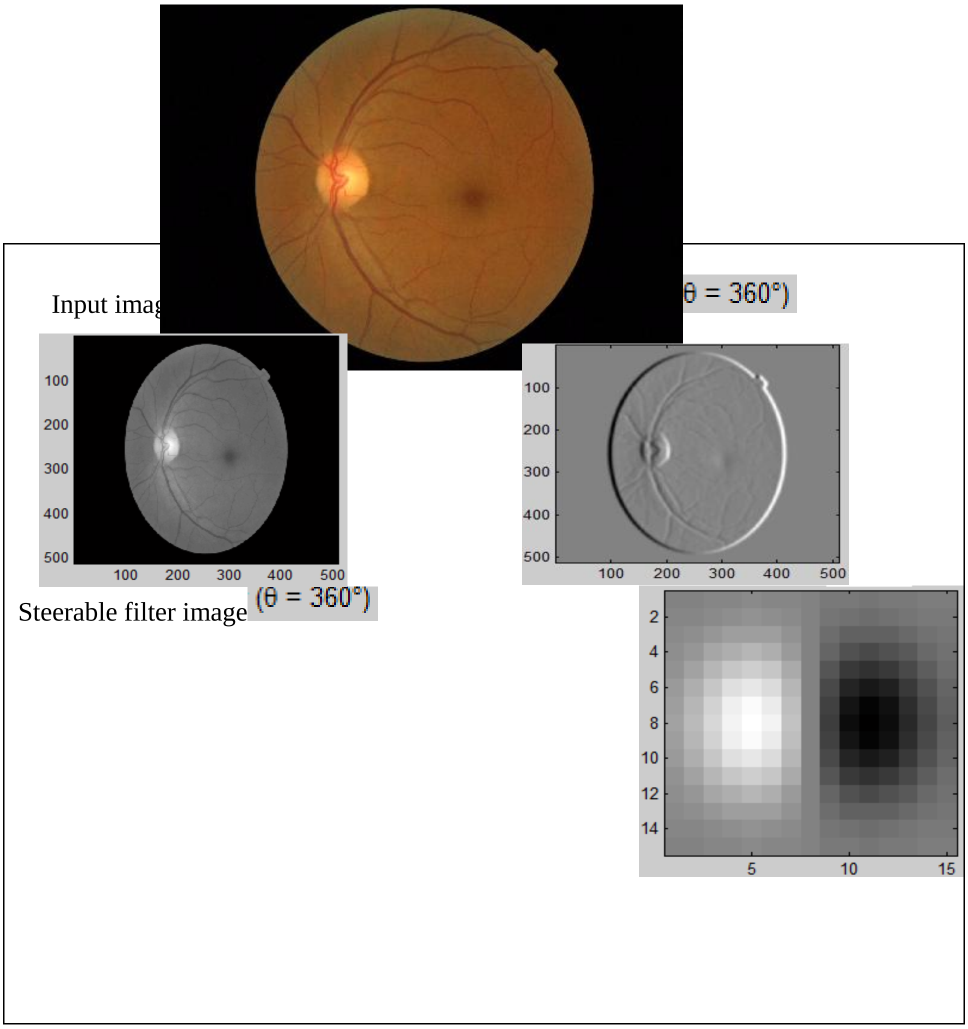

Here the input image and the corresponding gray scale image is obtained. The output image is delivered by using this filter image. It is rotated around 360 degeree and to get this above output image.

6. Conclusion

The main contribution of this technique was that to detect the large retinal hemorrhage detection in the fundus images. Algorithm for segmentation, extraction and classification has been presented. The severity level grading of diabetic retinopathy has been performed based on the International Clinical DR disease severity scale. The proposed algorithm extracts the noise from input images for easier segmentation process. The algorithms which are used to proposed the segmentation process was watershed transformation. Since the both normal and abnormal conditions was classified by using the classification algorithm based on input images. Finally, the number of locations of severity level has been graded into different images i.e., normal, mild, moderate ad severe. A comparison between the results of both the clinician's dataset and the input images has been done.The experiment results shows that to trained the classifier and the unseen large hemorrhages is to achieved by using splat feature classification. The boundaries of hemorrhages are preserved by using splat feature classification. An automated screening process for early diagnosis and intervention can hence be of great help to the patient and specialist alike in the timely management of this disease.

REFERENCES

[1] O. Faust, R. Acharya U., E. Y. K. Ng, K.-H. Ng, and J. S. Suri, "Algorithms for the automated detection of diabetic retinopathy using digital fundus images: A review," *J. Med. Syst.*, Apr2010 .

[2] M. Niemeijer, M. D. Abramoff, and B. van Ginneken, "Information fusion for diabetic retinopathy CAD in digital color fundus photographs," *IEEE Trans. Med. Imag.*, no. 5, pp. 775–785, May 2009.

[3] M. Niemeijer, B. van Ginneken, J. Staal, M. S. A. Suttorp-Schulten, and M. D. Abràmoff, "Automatic detection of red lesions in digital color fundus photographs," *IEEE Trans. Med. Imag.*, vol. 24, no. 5, 584-592,May 2005.

[4] G. Quellec, S. Russell, and M. Abràmoff, "Optimal filter framework for automated, instantaneous detection of lesions in retinal images," *IEEE Trans. Med. Imag.*, vol. 30, no. 2, pp. 523–533, Feb. 2011.

[5] Y. Hatanaka, T. Nakagawa, Y. Hayashi, M. Kakogawa, A. Sawada, K. Kawase, T. Hara, and H. Fujita, "Improvement of automatic hemorrhages detection methods using brightness correction on fundus images,"

in *Proc. SPIE*, 2008, vol. 6915, pp. 69 153E-1–69 153E-10.

[6] P. Jitpakdee, P. Aimmanee, and B. Uyyanonvara, "A survey on hemorrhage detection in diabetic retinopathy retinal images," in *Proc. 9th Int. Conf. Elect. Eng./Electron., Comput., Telecommun. Inf. Technol. (ECTI-CON)*, Bangkok, Thailand, 2012, pp. 1–4, vol.2.

[7] M. Abràmoff, M. Garvin, and M. Sonka, "Retinal imaging and image analysis," *IEEE Rev. Biomed. Eng.*, vol. 3, pp. 169–208, 2010.

[8] S. C. H. Hoi, R. Jin, J. Zhu, and M. R. Lyu, "Batch mode active learning and its application to medical image classification," in *Proc. ICML*, 2006, pp. 417–424.

[9] Fairfield, "Toboggan contrast enhancem ent for contrast segmentation," in *Proc. Int. Conf. Pattern Recognit.*, 1990, vol. 1, pp. 712–716.

[10] N. V. Chawla, N. Japkowicz, and A. Kotcz, "Editorial: Special issue on learning from imbalanced data sets," *SIGKDD Explorations*, no. 1, 1–6, 2004.

[11] C. L. Zitnick and S. B. Kang, "Stereo for image-based rendering using image over segmentation," *Int. J. Comput. Vis.*, no. 1, pp. 49–65, Feb. 2003.

[12] X. Ren and J. Malik, "Learning a classification model for segmentation," in *Int. Conf. Comput. Vis.*, 2003, vol. 1.

[13] Y.-C. Lin, Y.-P. Tsai, Y.-P. Hung, and Z.-C. Shih, "Comparison between immersionbased and toboggan based watershed image segmentation," *IEEE Trans. Image Process.*, no. 3, pp. 632–40, Mar.2006.

[14] G. Li, G. Liqun, P. Zhao-Yu, and W. Kun, "Image segmentation using multiscale gradient toboggan," in *Proc. 2nd IEEE Conf. Ind. Electron. Appl.*, May 2007, pp. 2206–2209.

[15] G. Quellec, M. Lamard, M. Abràmoff, E. Decencière, B. Lay, A. Erginay, B. Cochener, and G. Cazuguel, "A multiple instance learning framework for diabetic retinopathy screening," *Med. Image Anal*, vol. 16, no. 6, pp. 1228–40, 2012.

[16] M. Christopher, D. C. Moga, S. R. Russell, J. C. Folk, T. Scheetz, and M. Abràmoff, "Validation of tablet-based evaluation of color fundus images," *Retina*, vol. 32, no. 8, pp. 1.629–35,2003.

[17] M. Niemeijer, M. D. Abràmoff, and B. van Ginneken, "Fast detection of the optic disc and fovea in color fundus photographs," *Med. Image Anal.*, no. 6, pp. 859–870, Dec.2004.

[18] M. D. Abràmoff, W. L. M. Alward, E. C. Greenlee, L. Shuba, C. Y. Kim, J. H. Fingert, and Y. H. Kwon, "Automated segmentation of the optic disc from stereo color photographs using physiologically plausible features," *Invest. Ophthalmol. Vis. Sci.*, vol. 48, no. 4, pp. Apr. 2007.

[19] B. M. T. H. Romeny, Front-End Vision and Multi-Scale Image Anal-ysis: Multi-Scale Computer Vision Theory and Applications, Written in Mathematica. Berlin, Germany: Springer, 2003.

[20] L. Tang, M. Niemeijer, and M. Abràmoff, "Splat feature classification: Detection of the presence of large retinal hemorrhages," in *Proc. IEEE 8th Int. Symp. Biomed. Imag. (ISBI)*, 2011, pp. 681–684.

[21] M. Varma and A. Zisserman, "A statistical approach to texture classi-fication from single images," *Int. J. Comput. Vis.*, vol. 62, no. 1–2, pp. 61–81, 2005.

[22] T. Wagner, , B. Jahne, H. Haussecker, and P. Geissler, Eds., *Texture Analysis*. New York: Academic, 1999, vol. 2. 2005.